Filter bank canonical correlation analysis for implementing a high-speed SSVEP-based brain–computer interface

Filter bank canonical correlation analysis for implementing a high-speed SSVEP-based brain-computer interface

Xiaogang Chen[1], Yijun Wang[2,3], Shangkai Gao[1], Tzyy-Ping Jung[2], Xiaorong Gao[1]

[1] *Department of Biomedical Engineering, School of Medicine, Tsinghua University, Beijing, 100084 China*
[2] *Swartz Center for Computational Neuroscience, Institute for Neural Computation, University of California, San Diego, La Jolla, CA92093 USA*
[3] *State Key Laboratory on Integrated Optoelectronics, Institute of Semiconductors, Chinese Academy of Sciences, Beijing, 100083 China*

Email: yijun@sccn.ucsd.edu, gxr-dea@tsinghua.edu.cn

Abstract—

Objective. Recently, canonical correlation analysis (CCA) has been widely used in steady-state visual evoked potential (SSVEP)-based brain-computer interfaces (BCIs) due to its high efficiency, robustness, and simple implementation. However, the method to make use of harmonic SSVEP components to enhance the CCA-based frequency detection has not been well established. ***Approach.*** This study proposed a filter bank canonical correlation analysis (FBCCA) method to incorporate fundamental and harmonic frequency components to improve the detection of SSVEPs. A 40-target BCI speller based on frequency coding (frequency range: 8-15.8Hz, frequency interval: 0.2Hz) was used for performance evaluation. To optimize the filter bank design, three methods (M_1: sub-bands with equally spaced bandwidths; M_2: sub-bands corresponding to individual harmonic frequency bands; M_3: sub-bands covering multiple harmonic frequency bands) were proposed for comparison. Classification accuracy and information transfer rate (ITR) of the three FBCCA methods and the standard CCA method were estimated using an offline dataset from 12 subjects. Furthermore, an online BCI speller adopting the optimal FBCCA method was tested with a group of 10 subjects. ***Main results.*** The FBCCA methods significantly outperformed the standard CCA method. The method M_3 achieved the highest classification performance. At a spelling rate of ~33.3 characters per minute, the online BCI speller obtained an average ITR of 151.18±20.34 bits/min. ***Significance.*** By incorporating the fundamental and harmonic SSVEP components in target identification, the proposed FBCCA method significantly improves the performance of the SSVEP-based BCI, and thereby facilitates its practical applications such as high-speed spelling.

Keywords: Steady-state visual evoked potentials (SSVEP), brain-computer interface (BCI), harmonics, filter bank, canonical correlation analysis (CCA)

1.   Introduction

The steady-state visual evoked potentials (SSVEPs)-based brain-computer interface (BCI) has attracted more and more attention in the field of BCI due to its advantages such as high information transfer rate (ITR) and little user training (Wang et al., 2008; Vialatte et al., 2010). In a recent study (Chen et al., 2014), a 45-target SSVEP speller obtained an online ITR of 105 bits/min, showing its promising potential in high-speed communication. The high performance of an SSVEP BCI can be attributed to two factors: (1) a large number of classes, and (2) an efficient target identification method. In general, the BCI system with a high ITR is capable to provide a large number of selection options. In SSVEP BCIs, the multiple access (MA) technologies have been applied to coding multiple targets, leading to different system paradigms such as frequency coding, phase coding, and hybrid coding (Gao et al., 2014). Recent advances in generating visual flickers using monitor refresh rate make it possible to render a large number of flickers on a computer monitor (Wang et al., 2010; Nakanishi et al, 2014a, Chen et al., 2014). Using these methods, frequencies and phases of the flickers that can be realized are no longer limited by the refresh rate. The efficient coding techniques and robust stimulation presentation methods have significantly increased the number of classes in the SSVEP BCIs. For example, Chen et al. (2014) designed a 45-target speller based on frequency coding (7-15.8Hz with a step of 0.2Hz). In another study, Nakanishi et al. (2014b) implemented a 32-target speller using a mixed frequency and phase coding method (frequencies: 8-15Hz with an interval of 1Hz; phases: 0, 0.5π, π, 1.5π). The target identification method also plays an important role in system implementation. A BCI system with high ITR always shows high classification accuracy. In previous studies, advanced signal processing and machine learning techniques have been applied to the detection of SSVEPs. For example, spatial filtering approaches such as the canonical correlation analysis (CCA) (Lin et al., 2007) and minimum energy combination (MEC) (Friman et al., 2007) methods have been developed to enhance the SNR of SSVEPs. Recently, the CCA-based frequency detection method has been widely used due to its high efficiency, robustness, and simple implementation (Bin et al., 2009). In two recent studies, the SSVEP BCIs using the CCA-based method achieved high ITRs around 100 bits/min (Nakanishi et al., 2014a, Chen et al., 2014).

SSVEPs, which are also known as photic driving responses, can be characterized by sinusoidal-like waveforms at the stimulation frequency and its harmonic frequencies (Regan 1989). More specifically, SSVEPs consist of brain responses at frequencies identical, harmonic, and sub-harmonic to the stimulation frequency (Herrmann 2001). In addition to the fundamental frequency component, the harmonic components can provide useful information for frequency detection. The advantage of combining harmonic components in frequency detection has been demonstrated in previous studies (Müller-Putz et al., 2005; Wang et al., 2008). However, a solution to incorporate harmonic frequency components in the CCA-based frequency detection has not been well established. For example, Bin et al. (2009) compared different numbers of harmonic frequencies for the reference signals in CCA and showed no significant difference of classification accuracy. To extract the discriminative information embedded in the harmonic components of SSVEPs, a more efficient approach is required for the CCA-based frequency detection method. Filter bank analysis, which can decompose the SSVEPs into multiple sub-band components, might be a practical solution. In signal processing, filter bank methods have been widely used to analyze signals that exhibit multiple sub-band frequency components (Vetterli 1992; Boashash 2003). A filter bank indicates an array of band-pass filters that separates an input signal into multiple sub-band components. The filter bank method has been applied in recent BCI studies. For example, a filter bank common spatial pattern (FBCSP) method was proposed to extract EEG power features in mu and beta frequency bands and significantly improved the discrimination of different motor imagery states (Ang et al., 2012). To our knowledge, the filter bank method has not been reported in the SSVEP-based BCIs. Considering the distinct spectral properties of multiple harmonic frequencies in SSVEPs, the filter bank method has big potential to improve the CCA-based frequency detection of SSVEPs.

This study proposed a filter bank canonical correlation analysis (FBCCA) method to improve the frequency detection of SSVEPs. A 40-target BCI speller was implemented for performance evaluation. To avoid the use of harmonic frequencies as stimulus frequencies (e.g., 7Hz and 14Hz), the frequencies started from 8 to 15.8 Hz with a frequency interval of 0.2 Hz. This study first explored the amplitude and SNR of SSVEP components at fundamental and harmonic frequencies using an offline BCI experiment. Next, the proposed FBCCA method was employed to estimate BCI performance in offline analysis. To optimize the selection of sub-bands in a filter bank, three methods (M_1: sub-bands with equally spaced bandwidths; M_2: sub-bands corresponding to individual harmonic frequency bands; M_3: sub-bands covering multiple harmonic frequency bands) were proposed and compared with the standard CCA method. Finally, an online BCI experiment was conducted using the method M_3. The goal of this study was to demonstrate the efficacy of the FBCCA method in implementing a high-speed SSVEP-based BCI that does not require system calibration.

2. Methods

2.1 Visual speller design

2.1.1 Stimulus presentation

This study used a sampled sinusoidal stimulation method (Manyakov et al., 2013, Chen et al., 2014) to present visual flickers on a computer monitor. In general, the stimulus sequence $s(f, i)$ corresponding to frequency f can be generated by modulating the luminance of the screen using the following equation:

$$s(f, i) = \frac{1}{2}\{1 + \sin[2\pi f(i/\text{RefreshRate})]\} \tag{1}$$

where sin() generates a sine wave, and i indicates the frame index in the stimulus sequence. The dynamic range of the stimulation signal is from 0 to 1, where 0 represents dark and 1 represents the highest luminance. Theoretically, the flickering signal at any frequency (up to the half of the refresh rate) can be realized using refresh rate.

2.1.2 BCI speller

This study designed a 40-target BCI speller using a frequency coding approach (Middendorf et al., 2000, Cheng et al., 2002, Wang et al., 2006). As shown in figure 1(a), the user interface is a 5×8 stimulation matrix containing 40 characters (26 English alphabets, 10 digits, and four other symbols). 40 characters are tagged with equally spaced frequencies, of which the increment is proportional to the target index. Specifically, the frequency value for each character in the matrix can be obtained by:

$$f(k_x, k_y) = f_0 + \Delta f \times [(k_y - 1) \times 5 + (k_x - 1)], k_x \in [1\ 5], k_y \in [1\ 8]. \tag{2}$$

where k_x and k_y indicates the row and column index respectively. In this study, f_0 was 8Hz and Δf was 0.2Hz. Figure 1(b) illustrates the frequency values (i.e., 8-15.8Hz with an interval of 0.2Hz) for all characters.
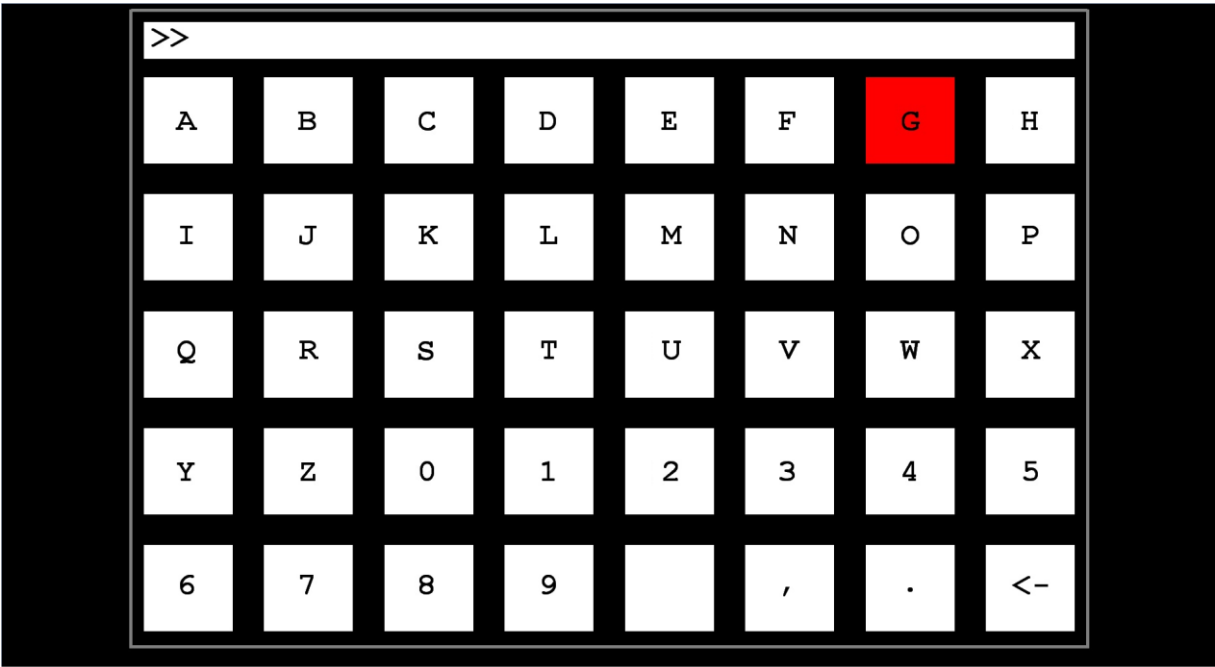
(a)
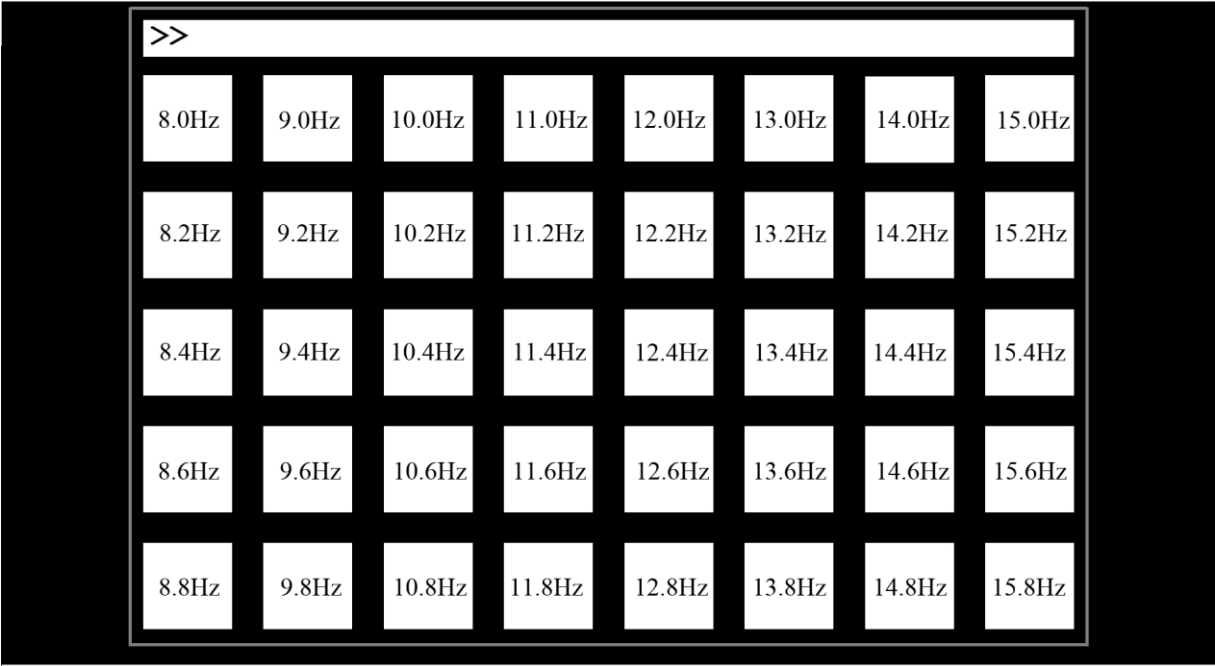
(b)

Figure 1. (a) The user interface of the 40-target BCI speller. The red square is an example of a visual cue indicating a target character 'G' in the BCI experiments. (b) The frequency values for all characters.

2.2 Filter bank canonical correlation analysis (FBCCA)

2.2.1 Standard CCA

CCA has been widely used to detect the frequency of SSVEPs (Lin et al., 2007; Bin et al., 2009; Chen et al., 2014). CCA is a statistical way used to measure the underlying correlation between two multi-dimensional variables. Considering two multi-dimensional variable X, Y and their linear combinations $x = X^T W_X$ and $y = Y^T W_Y$, CCA finds the weight vectors, W_X and W_Y, which maximize the correlation between x and y by solving the following problem:

$$\max_{W_X, W_Y} \rho(\pmb{x}, \pmb{y}) = \frac{E[\pmb{W}_X^T XY^T \pmb{W}_Y]}{\sqrt{E[\pmb{W}_X^T XX^T \pmb{W}_X]E[\pmb{W}_Y^T YY^T \pmb{W}_Y]}}. \tag{3}$$

The maximum of ρ with respect to $\pmb{W}_X$ and $\pmb{W}_Y$ is the maximum canonical correlation. In frequency detection of SSVEPs, $\pmb{X}$ indicates multi-channel SSVEPs and $\pmb{Y}$ refers to reference signals. To detect the frequency of SSVEPs in an unsupervised way, sinusoidal signals are used as the reference signals $\pmb{Y}_f$ (Lin et al., 2007):

$$\pmb{Y}_f = \begin{bmatrix} sin(2\pi ft) \\ cos(2\pi ft) \\ \vdots \\ sin(2\pi N_h ft) \\ cos(2\pi N_h ft) \end{bmatrix} \tag{4}$$

where f is the stimulation frequency and N_h is the number of harmonics. To recognize the frequency of SSVEPs, CCA calculates the canonical correlation between multi-channel SSVEPs and the reference signals corresponding to each stimulation frequency. The frequency of the reference signals with the maximal correlation is considered as the frequency of SSVEPs.

2.2.2 Filter bank CCA

This study proposed a FBCCA method to enhance the CCA-based frequency detection of SSVEPs. Figure 2 shows the flowchart of the proposed method. The FBCCA method consists of three major procedures: (1) filter bank analysis; (2) CCA between SSVEP sub-band components and sinusoidal reference signals; and (3) target identification. First, a filter bank analysis performed sub-band decompositions with multiple filters that have different pass-bands. In this study, the band-pass filters for extracting sub-band components ($\pmb{X}_{SB_n}, n = 1,2,...,N$) from original EEG signals $\pmb{X}$ were zero-phase Chebyshev Type I Infinite Impulse Response (IIR) filters. The filtering was implemented using the filtfilt() function in MATLAB (MathWorks, Inc.). After the filter bank analysis, the standard CCA process was applied to each of the sub-band components separately, resulting in correlation values between the sub-band components and the predefined reference signals corresponding to all stimulation frequencies ($\pmb{Y}_{f_k}, k = 1,2,...,40$). For the kth reference signals, a correlation vector $\pmb{\rho}_k$ consisting of N correlation values was defined as follows:

$$\pmb{\rho}_k = \begin{bmatrix} \rho_k^1 \\ \rho_k^2 \\ \vdots \\ \rho_k^N \end{bmatrix} = \begin{bmatrix} \rho\big(\pmb{X}_{SB_1}{}^T \pmb{W}_X(\pmb{X}_{SB_1}\pmb{Y}_{f_k}), \pmb{Y}^T \pmb{W}_Y(\pmb{X}_{SB_1}\pmb{Y}_{f_k})\big) \\ \rho\big(\pmb{X}_{SB_2}{}^T \pmb{W}_X(\pmb{X}_{SB_2}\pmb{Y}_{f_k}), \pmb{Y}^T \pmb{W}_Y(\pmb{X}_{SB_2}\pmb{Y}_{f_k})\big) \\ \vdots \\ \rho\big(\pmb{X}_{SB_N}{}^T \pmb{W}_X(\pmb{X}_{SB_N}\pmb{Y}_{f_k}), \pmb{Y}^T \pmb{W}_Y(\pmb{X}_{SB_N}\pmb{Y}_{f_k})\big) \end{bmatrix} \tag{5}$$

where $\rho(x, y)$ indicates the correlation coefficient between x and y. A weighted sum of squares of the correlation values corresponding to all sub-band components (i.e., $\rho_k^1, ..., \rho_k^N$) was calculated as the feature for target identification:

$$\tilde{\rho}_k = \sum_{n=1}^{N} \pmb{w}(n) \cdot (\rho_k^n)^2 \tag{6}$$

where n is the index of the sub-band. According to the finding that the SNR of SSVEP harmonics decreases as the response frequency increases (see Section 3. 1), the weights for the sub-band components were defined as follows:

$$\pmb{w}(n) = n^{-a} + b, n \in [1 \ N] \tag{7}$$

where a and b are constants that maximize the classification performance. In practice, a and b can be determined using a grid search method using an offline analysis. Finally, $\tilde{\rho}_k$ corresponding to all stimulation frequencies (i.e., $\tilde{\rho}_1, ..., \tilde{\rho}_{40}$) were used for determining the frequency of SSVEPs. The frequency of the reference signals with the maximal $\tilde{\rho}_k$ is considered as the frequency of SSVEPs.
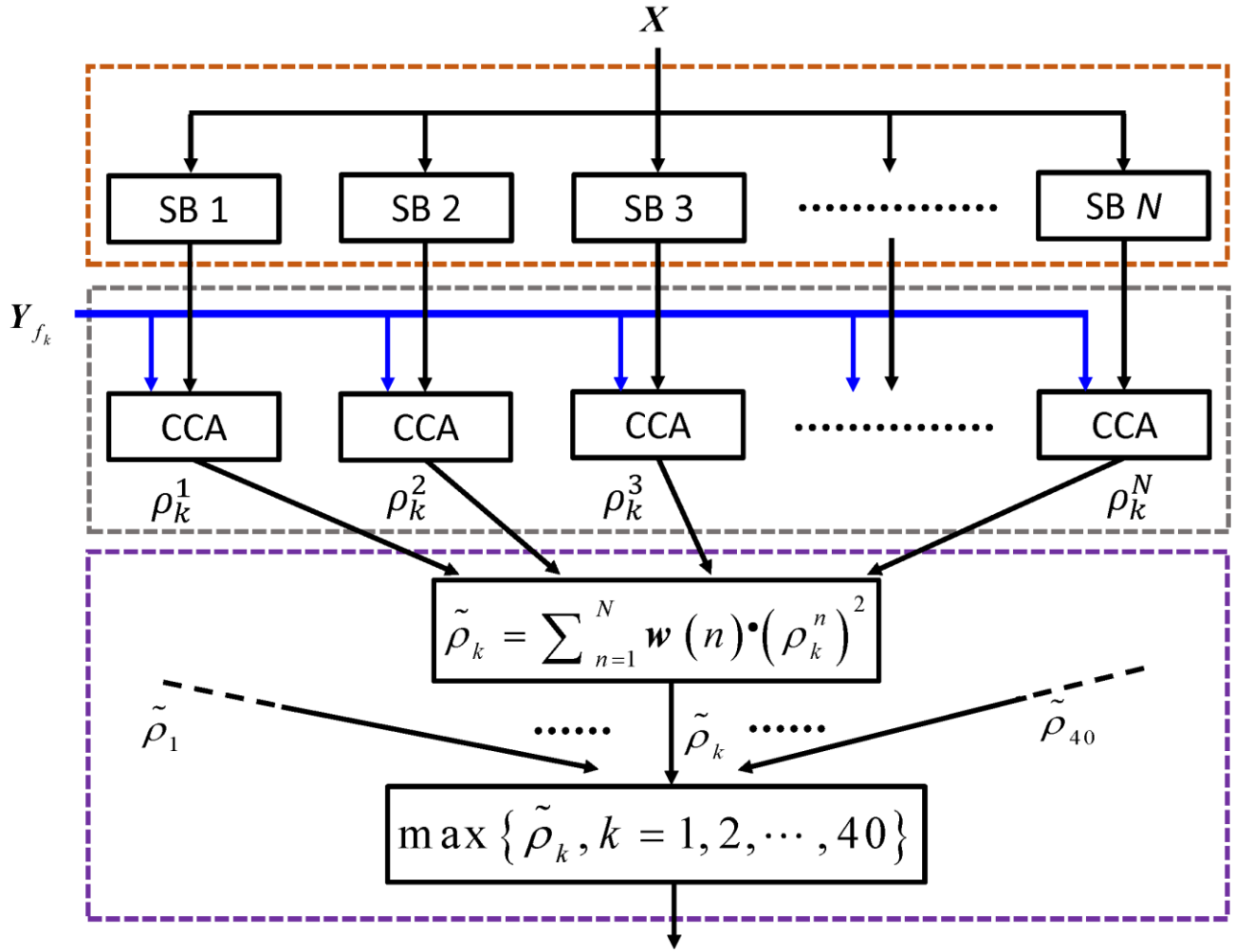
Figure 2. Flowchart of the FBCCA method for frequency detection of SSVEPs.

2.2.3 Filter bank design

The bandwidth of the stimulation frequencies (8-15.8Hz) was 8Hz in this study. According to the SNR analysis of SSVEP components in this study (see Section 3.1), the fundamental and harmonic SSVEP components exhibited high SNR within the frequency band from the stimulation frequency to an upper-bound frequency around 90Hz. Therefore, the frequency range within [8Hz 88Hz] (i.e., 10 times of the bandwidth of the stimulation frequencies) was selected for the filter bank. In practice, the frequency range of the filter bank can be further optimized towards the highest BCI performance.

The goal of filter bank analysis is to decompose SSVEPs into sub-band components so that independent information embedded in the harmonic components can be extracted more efficiently than the standard CCA method. This study proposed three methods for designing sub-bands in the filter bank. The first method (M_1) divided the full frequency band of SSVEP components into sub-bands with equally spaced bandwidths (i.e., the bandwidth of the stimulation signals). As shown in figure 3(a), M_1 divided the frequency band of [8Hz 88Hz] into 10 sub-bands, each of which has a bandwidth of 8Hz in this study. The second method (M_2) designed sub-bands corresponding to individual harmonic frequency bands. In this study, the nth sub-band started from the frequency at $n \times 8$ Hz, and ended at the minimum value between $n \times 16$ Hz and 88Hz (see figure 3(b)). The third method (M_3) generated sub-bands covering multiple harmonic frequency bands with a high cutoff frequency at the upper-bound frequency of the SSVEP components. As shown in figure 3 (c), the nth sub-band started from the frequency at $n \times 8$ Hz and ended at 88Hz. In the implementation of band-pass filtering, an additional bandwidth of 2Hz was added to both sides of the passband for each sub-band. For example, the passband of the first sub-band in M_1 was set to [6Hz 18Hz].
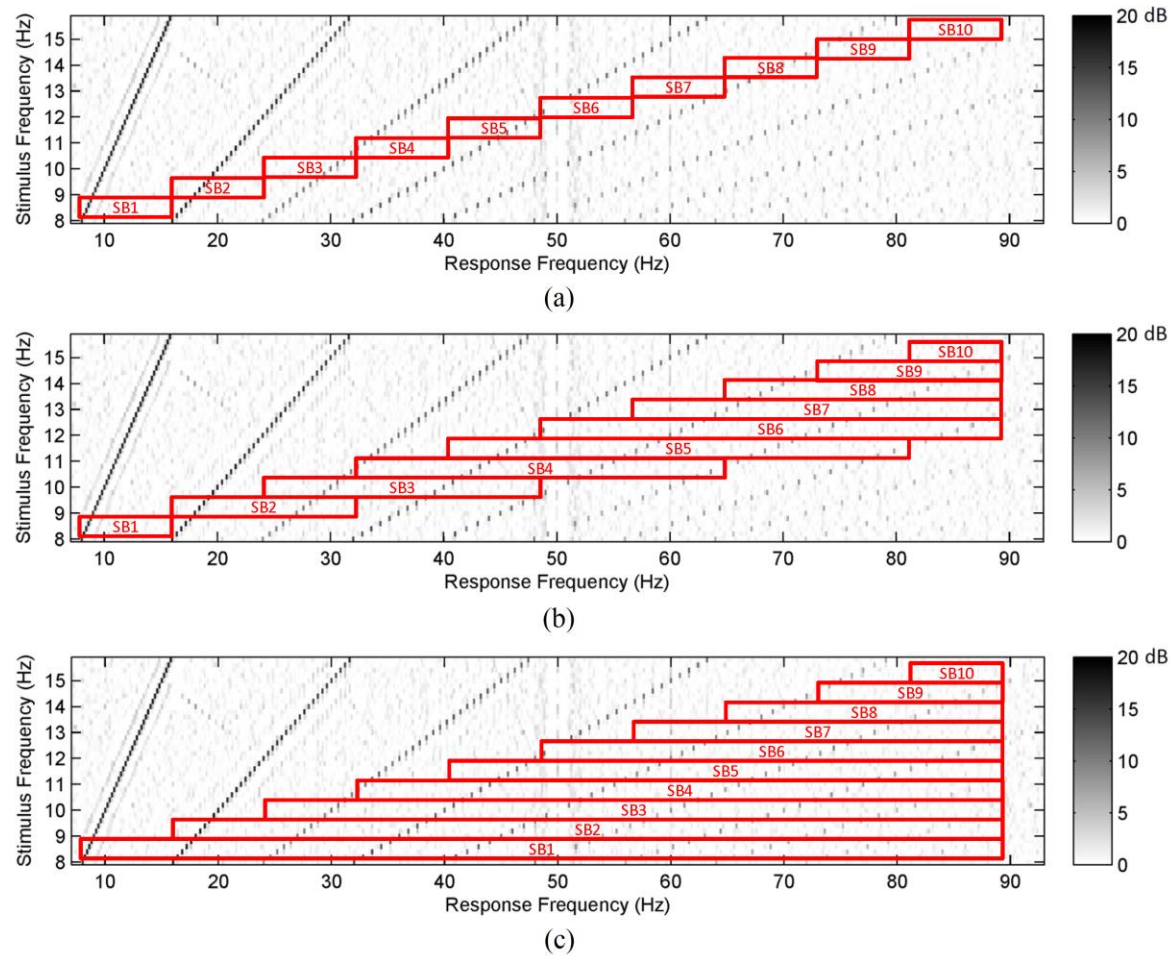
Figure 3. Frequency selection for all sub-bands in filter bank design for the three FBCCA methods: (a) M_1, (b) M_2, and (c) M_3. The background image shows the SNR of SSVEPs as a function of stimulation frequency and response frequency (see details in Section 3.1).

2.3 Data acquisition

This study designed an offline and an online BCI experiment using the SSVEP-based BCI speller. Nineteen healthy subjects (10 females, aged 22-30 years, mean age: 25 years) with normal or corrected-to-normal vision participated in the experiment. The offline and online experiments were carried out separately with a 2-month interval. Among all the subjects, 12 subjects participated in the offline experiment. Since nine of the 12 subjects who participated in the off-line experiments were not available during the online experiments, we recruited additional seven subjects for the online experiment. That is, three subjects (S1, S5, and S9, highlighted in table 1) participated in both experiments. Each participant was asked to read and sign an informed consent form before the experiment.

During the experiment, EEG data were acquired using a Synamps2 system (Neuroscan, Inc.) at a sampling rate of 1,000Hz. Nine electrodes over the parietal and occipital areas (Pz, PO5, PO3, POz, PO4, PO6, O1, Oz, and O2) were used to record SSVEPs. The electrode locations were selected toward high classification performance in a separate study using a 64-channel data set. The reference electrode was placed at the vertex. Electrode impedances were kept below 10kΩ. To remove the common power-line noise, a notch filter at 50Hz was applied in data recording. Event triggers generated by the stimulus program were sent from the parallel port of the computer to the amplifier and recorded on an event channel synchronized to the EEG data. In the online experiment, EEG data and trigger signals were recorded and analyzed by the online data analysis program in real time. The online data analysis program was developed under MATLAB.

The stimulation matrix of the BCI speller (see figure 1(a)) was presented on a 23.6-inch LCD screen with a resolution of 1920×1080 pixels and a refresh rate of 60Hz. Each stimulus was rendered within a 140×140 pixels square. The vertical and horizontal distances between two neighboring stimuli were 50 pixels. The stimulus program was developed under

MATLAB using the Psychophysics Toolbox Version 3 (Brainard 1997). During the experiment, subjects were seated in a comfortable chair in a dimly lit soundproof room at a viewing distance of approximately 70cm from the monitor.

2.3.1 Offline experiment

The offline BCI experiment consisted of six blocks. Each block contained 40 trials corresponding to all 40 characters presented in a random order. Each trial started with a visual cue (a red square, see figure 1(a)) indicating a target stimulus. The cue appeared for 0.5s on the screen. Subjects were asked to shift their gaze to the target as soon as possible within the cue duration. Following the cue offset, all stimuli started to flicker on the screen concurrently and lasted 5s. After stimulus offset, the screen was blank for 0.5s before the next trial began, which allowed the subjects to have short breaks between consecutive trials. Each trial lasted a total of 6s. To facilitate visual fixation, a red triangle appeared below the flickering target during the stimulation period. In each block, subjects were asked to avoid eye blinks during the stimulation period. To avoid visual fatigue, there was a rest for several minutes between two consecutive blocks.

2.3.2 Online experiment

The online BCI experiment consisted of five blocks; each including 40 trials. The parameters in the FBCCA method were optimized based on the offline analysis with the dataset from the offline experiment (see details in Section 3.2.2). Each trial only lasted 1.8s, including 1.25s for visual stimulation and 0.55s for gaze shifting. The cue for next target appeared right after the stimulus offset. Visual and auditory feedbacks were provided to the subjects in real time. A short beep was sounded after a target was correctly identified by the online data analysis program. At the same time, the target character was typed in the text input field on the top of the screen (see figure 1(a)). In the online experiment, the BCI system spelled at a rate of ~33.3 characters per minute (i.e., 1.8 seconds per character).

2.4 Data analysis

2.4.1 Data preprocessing

In offline and online experiments, data epochs comprising nine-channel SSVEP signals were extracted according to event triggers generated by the stimulus program. Considering a latency delay in the visual system (Russo and Spinelli, 1999), the data epochs for offline and online experiments were extracted in [0.14s 5.14s] and [0.14s 1.39s] respectively (time 0 indicated stimulus onset). In this study, the 140ms latency delay was selected towards the highest classification accuracy in the offline experiment across all subjects. To reduce the computation and memory costs, all data epochs were down-sampled to 250Hz.

2.4.2 Amplitude and signal to noise ratio (SNR) of SSVEPs

This study analyzed the amplitude and SNR of SSVEP components using the five-second long epochs from the offline experiment. The amplitude spectrum $y(f)$ was calculated by fast Fourier Transform (FFT). SNR in decibels (dB) was defined as the ratio of $y(f)$ to the mean value of the ten neighboring frequencies (i.e., five frequencies on each side):

$$\text{SNR} = 20 \log_{10} \frac{y(f)}{\sum_{k=1}^{5}[y(f-0.2\times k)+y(f+0.2\times k)]} \tag{8}$$

For SSVEPs at each stimulation frequency, the amplitude spectrum was estimated by averaging across the amplitude spectra corresponding to nine channels, six blocks, and 12 subjects. SNR was then calculated using the mean amplitude spectrum. To better illustrate the characteristics of SSVEP harmonic components, this study generated images of amplitude and SNR as a function of stimulation frequency and response frequency (Herrmann 2001).

2.4.3 SSVEP detection using FBCCA

This study investigated the performance of the proposed three FBCCA methods with the offline dataset and selected the optimal method for the online BCI experiment. The data length for the online experiment was set to 1.25s, which led to the highest ITR in offline analysis. To quantify BCI performance using the FBCCA method, the following parameters need to be optimized for the online BCI experiment. The first parameter is the number of harmonics for the sinusoidal reference signals in the standard CCA process (i.e., N_h in (4)). The second parameter is the weight vector for the sub-band components (i.e., w in (7)). The third parameter is the number of sub-bands in the filter bank (i.e., N in (6)). These parameters might interact with each other in the estimation of BCI performance. For simplicity, this study determined these parameters in two steps. N_h was

first selected by comparing BCI performance using different numbers from 1 to 10 with the standard CCA method. For each of the FBCCA methods, w and N were then determined by a grid search method where a, b, and N were limited to [0:0.25:2], [0:0.25:1], and [1:1:10] respectively. The parameters that led to the highest ITR were selected for SSVEP detection in the online experiment.

2.4.4 Performance evaluation

To evaluate performance of the proposed method, classification accuracy and ITR (Wolpaw et al., 2002) were calculated for the online and offline experiments separately. The data length corresponding to the highest ITR (i.e., 1.25s) was selected for evaluating BCI performance using different parameters. For the offline experiment, results for the three FBCCA methods and the standard CCA method were calculated for comparison. This study also calculated accuracy and ITR with different data lengths (from 0.25s to 3.5s with a step of 0.25s) for the FBCCA method M_3 and the standard CCA method. The parameters, which resulted in the highest ITR, were selected for the online experiment. For the online experiment, classification accuracy and ITR were calculated by the online data analysis program using the method M_3. For the estimation of ITR in both offline and online experiments, the 0.55s gaze shifting time was included in the calculation of ITR. In this study, the spelling rate of the BCI speller was 1.8 seconds per selection.

2.4.5 Statistic analysis

In this study, statistical analyses were conducted using SPSS software (IBM SPSS Statistics, IBM Corporation). One-way repeated-measures analysis of variance (ANOVA) was used to test the difference of classification accuracy between different numbers of Nh (i.e., number of harmonics in (4)) and N (i.e., number of sub-bands in (5)) respectively. The Greenhouse-Geisser correction was applied if the data did not conform to the sphericity assumption by Mauchly's Test of Sphericity. All post-hoc pairwise comparisons were Bonferroni corrected. The alpha level was set at 0.05.

3. Results

3.1 Amplitude and SNR of SSVEPs

For each stimulation frequency, the amplitude spectrum of SSVEPs was estimated by averaging across nine channels, six blocks and 12 subjects in the offline experiment. Figure 4(a) shows the mean amplitude spectrum of SSVEPs at 15Hz. The fundamental component at 15Hz showed the highest amplitude (1.93uV). The amplitude of harmonics dropped significantly as the response frequency increased (1st harmonic: 0.74uV, 2nd harmonic: 0.33uV, 3rd harmonic: 0.19uV, 4th harmonic: 0.12uV, 5th harmonic: 0.07uV). To be noticed, the amplitude of background EEG activities also decreased as the frequency increased. This character resulted in relatively high SNR for harmonics in the high frequency band. Figure 4(b) shows the corresponding SNR of SSVEPs at 15Hz. The bandwidth of neighboring frequencies was set to 2Hz (i.e., [f-1 f+1], see (8)). Although the amplitude of harmonics was much lower than the fundamental component, the SNRs decreased slowly and steadily following the increase of frequency (fundamental: 16.61dB, 1st harmonic: 14.69dB, 2nd harmonic: 12.68dB, 3rd harmonic: 10.89dB, 4th harmonic: 8.80dB, 5th harmonic: 5.43dB). This property was also applicable to other stimulation frequencies. Figure 5 shows the amplitude and SNR for all stimulation frequencies as functions of stimulation frequency and response frequency (Herrmann 2001). The SSVEP harmonics with frequencies up to 90Hz are clearly shown in the SNR image. For example, the fundamental component and nine harmonics can be observed for SSVEPs corresponding to the stimulation frequencies below 9Hz (see figure 5(b)). Since the classification performance highly correlates with the SNR but not the amplitude of SSVEPs, the SSVEP harmonics can provide rich and robust information for target identification.
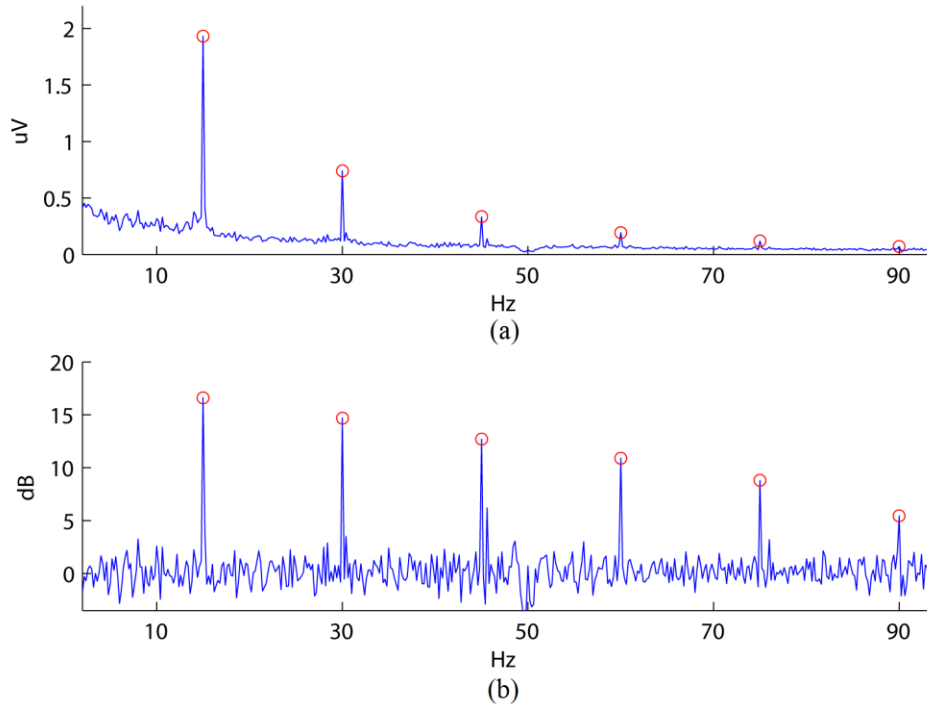
Figure 4. (a) Amplitude spectrum and (b) SNR of SSVEPs at 15Hz. The circles indicate the fundamental and harmonic frequencies of 15Hz (i.e., 15Hz, 30Hz, 45Hz, 60Hz, 75Hz, and 90Hz).
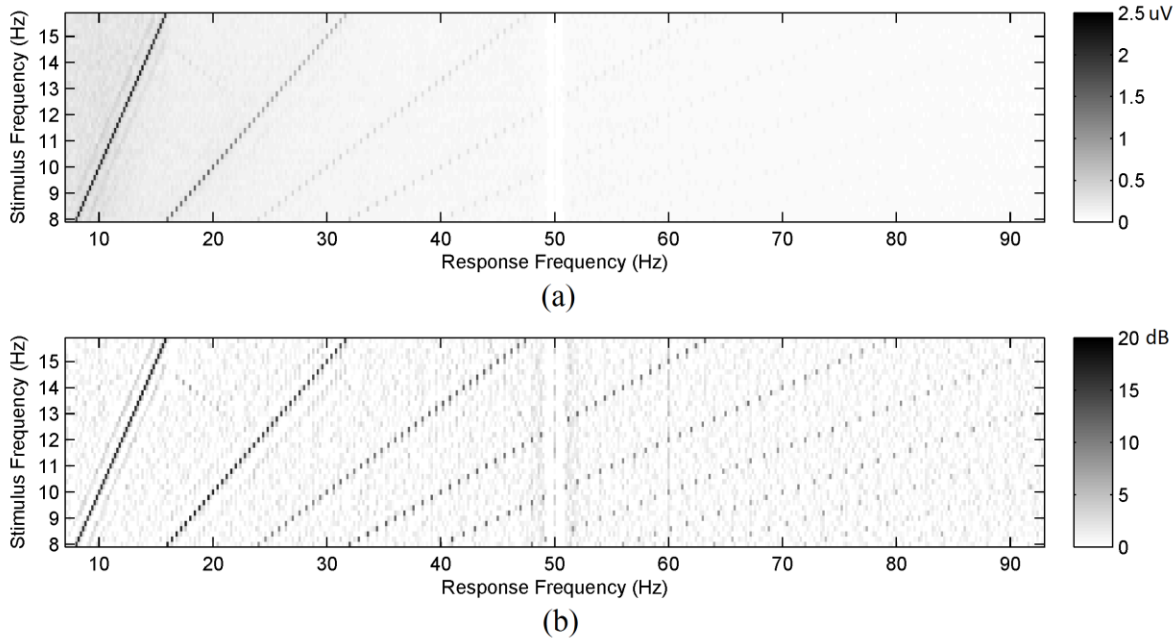
Figure 5. (a) Amplitude spectra and (b) SNRs for all stimulation frequencies as functions of stimulation frequency and response frequency. The frequency interval in the images was 0.2Hz. The sudden drop at 50Hz was caused by the notch filter used for removing power line noise in data recording.

3.2 Offline analysis on BCI performance

3.2.1 Standard CCA

Figure 6(a) shows the classification accuracy of the standard CCA method corresponding to different data lengths (from 0.25 s to 3.5 s with a step of 0.25 s) and different numbers of harmonics in the reference signals (i.e., N_h in (4)). Figure 6(b) details the classification accuracy with a data length of 1.25s, which was used in the online experiment. Overall, the classification

accuracy increased when the number of harmonics increased. One-way repeated-measures ANOVA showed that there was significant difference between different numbers of harmonics in the standard CCA method ($F_{(9,99)}$=29.16, $p<0.05$). Pairwise comparisons revealed significant difference between Nh=1 and all the other Nh values (Nh=1: 54.16%, Nh=2: 71.18%, Nh=3: 74.89%, Nh=4: 76.35%, Nh=5: 76.80%, Nh=6: 76.94%, Nh=7: 77.11%, Nh=8: 77.04%, Nh=9: 77.04%, Nh=10: 76.97%). There was also a significant difference between Nh=3 and Nh=5. These results indicate the selection of N_h plays an important role in the standard CCA method. The involvement of harmonic frequencies in the reference signals can improve the performance of the standard CCA method.
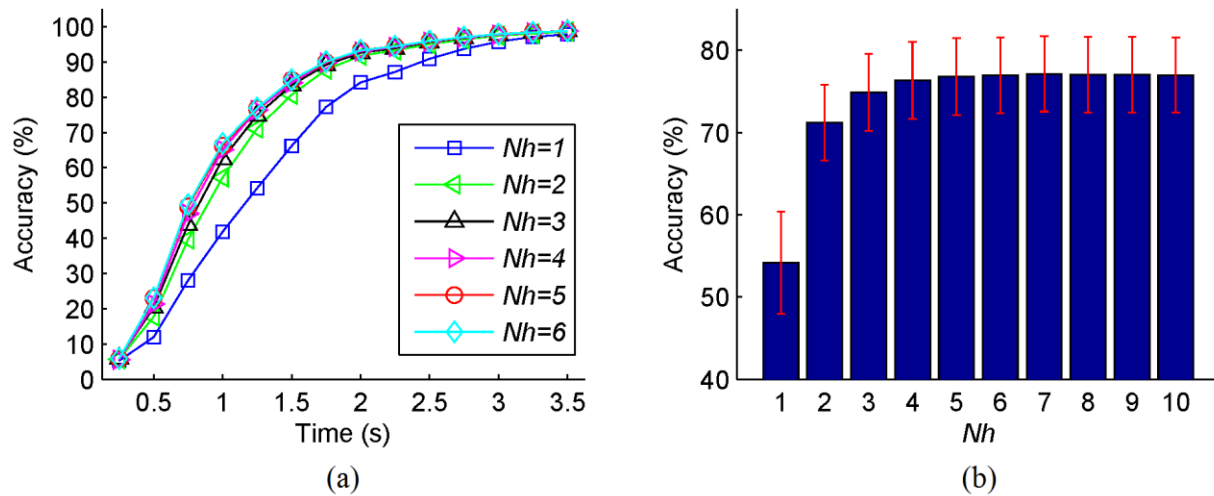

Figure 6. (a) Classification accuracy with different data lengths (from 0.25s to 3.5s with a step of 0.25s) using different numbers of harmonics in the standard CCA method. (b) Classification accuracy with a data length of 1.25s. The error bars represent standard errors.

3.2.2 FBCCA

The classification results from the standard CCA method showed significant improvements while Nh increased from 1 to 5 (see figure 6). This study further compared Nh=1 to 10 together with the parameters that maximized the simulated ITR in the offline analysis. One-way repeated-measures ANOVA showed that there was significant difference between different numbers of harmonics (M_1: $F_{(9,99)}$=36.59, $p<0.05$; M_2: $F_{(9,99)}$=46.81, $p<0.05$; M_3: $F_{(9,99)}$=34.59, $p<0.05$). For the M_1 method, pairwise comparisons revealed significant differences ($p<0.05$) between Nh=1 and all the other Nh values, between Nh=2 and Nh values (4-6), and between Nh=3 and Nh values (4-6). For the M_2 method, significant differences ($p<0.05$) were found between Nh=1 and all the other Nh values, between Nh=2 and Nh values (4-7), and between Nh=3 and Nh values (4, 5). For the M_3 method, significant differences ($p<0.05$) were found between Nh=1 and all the other Nh values, between Nh=2 and Nh values (4-6), and between Nh=3 and Nh=5. All three FBCCA methods obtained the highest classification accuracy when Nh=5. Therefore, this study used Nh=5 for all standard CCA processes in the FBCCA methods.

As described in Section 2.4.3, a grid search was applied to determine the optimal parameters for FBCCA method. The grid search involved the simultaneous optimization of the weight vector w (i.e., a and b) and the number of sub-bands N. Figure 7 shows the maximal classification accuracy (figure 7(a)-(c)) and the corresponding N values (figure 7(d)-(f)) with different a and b for the three FBCCA methods separately with a data length of 1.25s. The optimal a and b values for the three methods showed slight differences (M_1: (1.75, 0.25), M_2: (1.25, 0.25), M_3: (1.25, 0.25)). The corresponding N values were also different (M_1: 8, M_2: 8, M_3: 7). Figure 8 shows the classification accuracy and simulated ITR for the three FBCCA methods using different N values from 1 to 10. When the number of sub-bands increased, the accuracy and ITR of the FBCCA methods increased significantly to the peak performance at different N values (M_1: 8, M_2: 8, M_3: 7) and then decreased slightly. This finding suggests that the involvement of the sub-bands in the very high frequency range (e.g., the 9th and 10th sub-bands), which showed relatively low SNR, does not improve the overall classification performance. One-way repeated-measures ANOVA showed significant difference of accuracy between different numbers of sub-bands for the three FBCCA methods (M_1: $F_{(9,99)}$=36.66, $p<0.05$; M_2: $F_{(9,99)}$=43.75, $p<0.05$; M_3: $F_{(9,99)}$=23.61, $p<0.05$). For the M_1 method, pairwise comparisons revealed significant differences ($p<0.05$) between N=1 and all the other N values, between N=2 and N values (5-10), between N=3 and N values (6-10), between N=4 and N values (5-10), and between N=5 and N values (6-10). For the M_2 method, significant differences ($p<0.05$) were found between N=1 and all the other N values, between N=2 and N values (3-10), between N=3 and N values (4-10), between N=4 and N values (5-9), and between N=5 and N values (6-8). For the M_3 method, significant differences ($p<0.05$) were found between N=1 and N values (3-10), between N=2 and N values (4, 6-9),

and between $N=3$ and N values (4-8). All three FBCCA methods obtained much higher peak accuracy than the standard CCA method (M_1: 83.71%, M_2: 87.15%, M_3: 89.47%, standard CCA: 76.80%). Paired t-tests showed significant difference of classification accuracy between the FBCCA methods and the standard CCA method (M_1 vs. CCA: $p<0.01$; M_2 vs. CCA: $p<0.001$; M_3 vs. CCA: $p<0.001$). For the FBCCA method, M_3 and M_1 showed the highest and the lowest peak accuracy respectively. The difference of peak accuracy between the three FBCCA methods was also significant (M_1 vs. M_2: $p<0.001$; M_1 vs. M_3: $p<0.001$; M_2 vs. M_3: $p<0.01$). The resulting peak ITR for the FBCCA methods were consistently higher than the standard CCA method (M_1: 130.72 bits/min, M_2: 139.44 bits/min, M_3: 145.52 bits/min, standard CCA: 113.85 bits/min). To be noticed, when the number of sub-bands is 1, the method M_3 is the same as the standard CCA method.
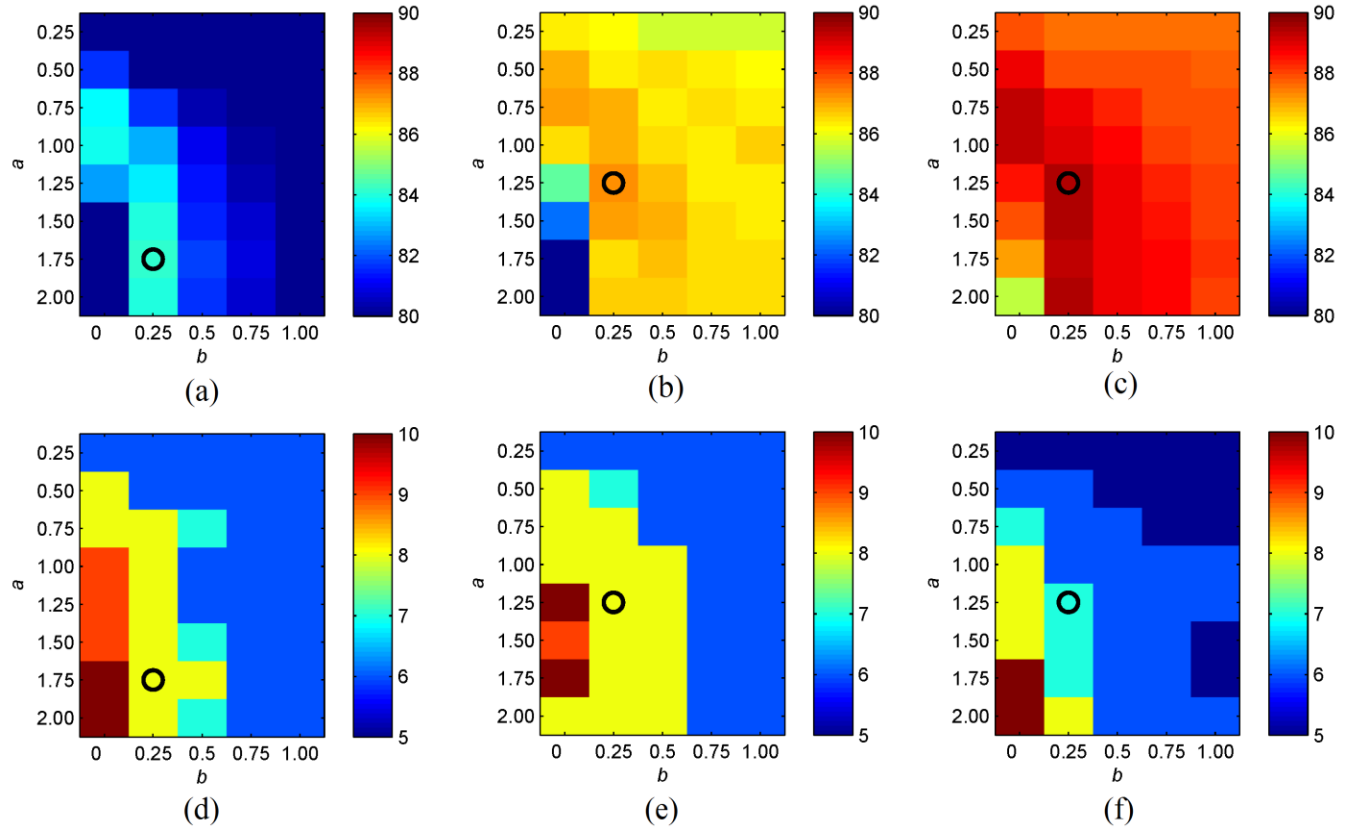

Figure 7. Maximum classification accuracy (%) in the grid search of the weight vector $\boldsymbol{w}$ in the FBCCA methods: (a) M_1, (b) M_2, (c) M_3 and the corresponding N values (i.e., number of sub-bands): (d) M_1, (e) M_2, (f) M_3. The black circles indicate the location of the maximum accuracy among different combinations of a and b.

(a)   (b)
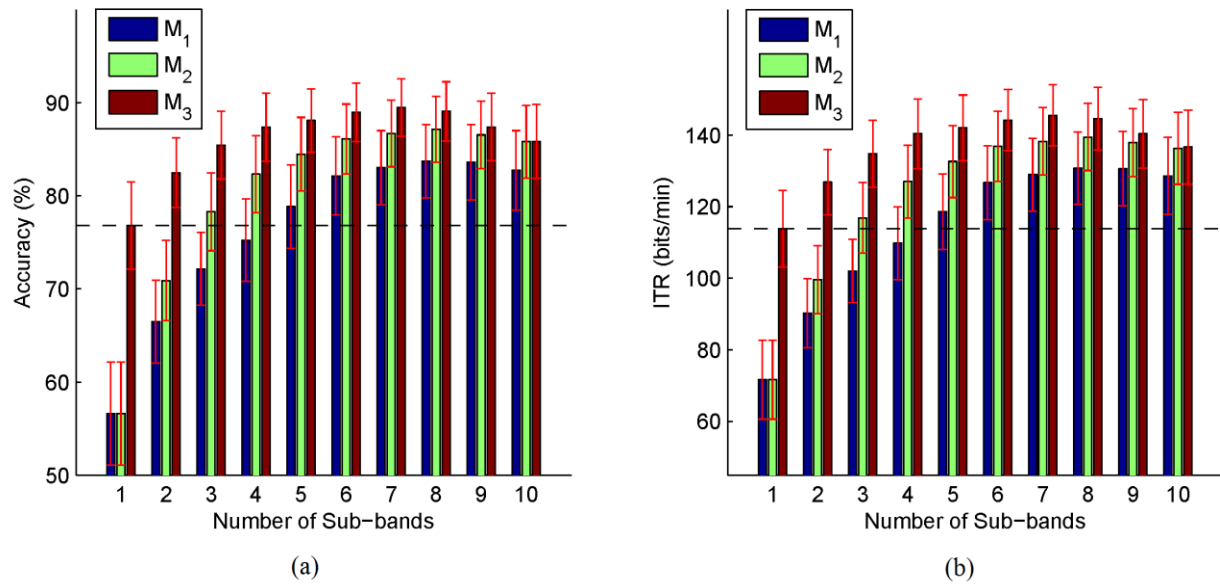
Figure 8. (a) Classification accuracy and (b) ITR for the FBCCA methods using different number of sub-bands from 1 to 10. The data length of SSVEPs was 1.25s. The dash lines indicate accuracy (76.80%) and ITR (113.85 bits/min) for the standard CCA method.

Figure 9 illustrates BCI performance for the FBCCA method M_3 and the standard CCA method as a function of different data lengths of SSVEPs (from 0.25s to 3.5s with a step of 0.25s). M_3 outperform the standard CCA method for all different data lengths, with more significant differences in accuracy and ITR between 0.5s and 2.25s ($p<0.01$). When the data length reached 2.5s, the accuracy for both methods was higher than 95%, showing no significant difference between the two methods. The data length corresponding to the highest ITR for M_3 (i.e., 145.52 bits/min) was 1.25s. In this study, the data length of 1.25s was thus selected for the online BCI experiment towards a high ITR. In contrast, the standard CCA method obtained a much lower ITR with very significant difference (113.85 bits/min, $p<0.0001$).

(a)   (b)
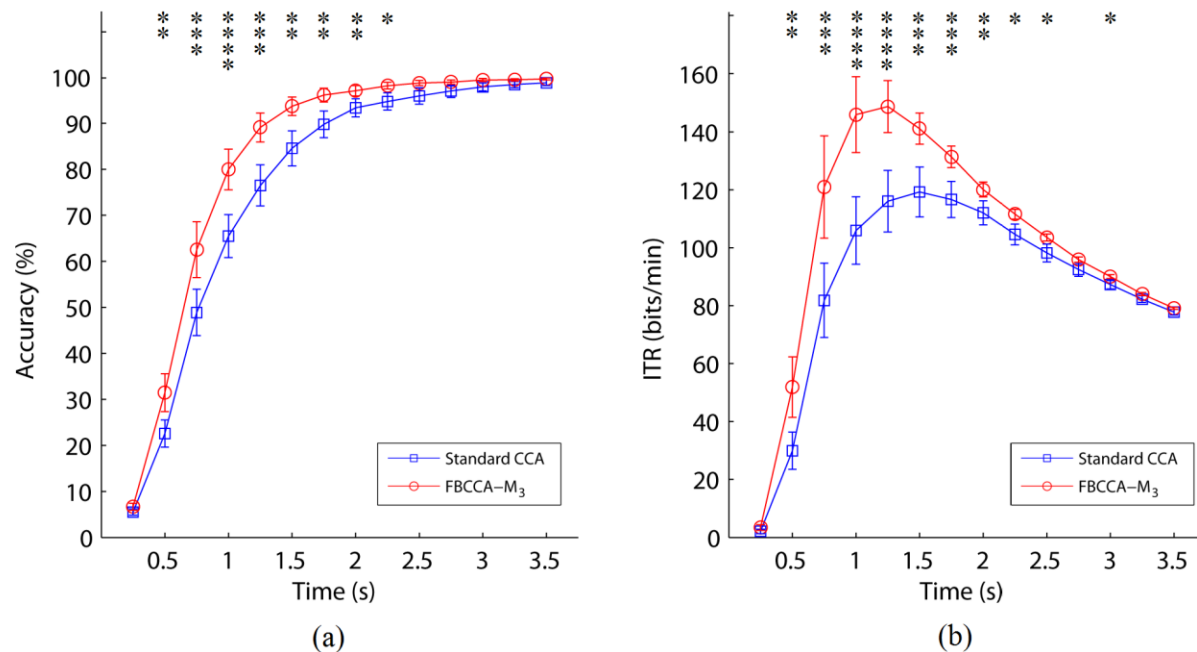
Figure 9. (a) Classification accuracy and (b) ITR for the FBCCA method M_3 and the standard CCA method using different data lengths (from 0.25s to 3.5s with a step of 0.25s). The error bars indicate standard errors. The asterisks indicate significant difference between the two methods (*: $p < 0.05$, **: $p < 0.01$, ***: $p < 0.001$, ****: $p < 0.0001$).

3.3 Online BCI performance

Table 1 lists the accuracy and ITR for all subjects in the online BCI experiment. Subjects S1, S5, and S9 (highlighted in table 1) also participated in the offline experiment. The online BCI system spelled at a speed of 33.3 characters per minute (i.e., 1.8 seconds per character). The average accuracy was $91.95 \pm 7.22\%$ across all subjects, leading to an average ITR of 151.18 ± 20.34 bits/min. For all individuals, the minimal and maximal ITR was 114.48 bits/min (Subject S10) and 175.00 bits/min (Subject S1) respectively. The online accuracy and ITR were comparable to those obtained in the offline experiments (accuracy: 89.47%, ITR: 145.52 bits/min). The slight difference could be due to different groups of subjects in the offline and online experiments (see Section 2.3) and the effect of feedback on performance. Paired t-tests showed there was no significant difference of classification accuracy and ITR between online and offline experiments for the three subjects who participated in both experiments ($p > 0.05$). Note that, the comparable performance obtained in the online experiment further proved the generalization ability of the parameters optimized in the offline analysis. For comparison, this study further calculated the BCI performance of the online data using the standard CCA method. The results showed that the FBCCA method (accuracy: 91.95%, see table 1) significantly outperformed the standard CCA methods using different numbers of harmonics (Nh=1: 58.85%, Nh=2: 74.50%, Nh=3: 77.65%, Nh=4: 79.60%, Nh=5: 80.40%, Nh=6: 80.60%, Nh=7: 81.00%, Nh=8: 80.85%, Nh=9: 80.90%, Nh=10: 80.85%; $p < 0.05$). There was no significant difference between Nh values from 5 to 10 for the standard CCA method ($p > 0.05$). These results demonstrated the efficacy and feasibility of the FBCCA method in an online SSVEP-based BCI.

Table 1. Classification accuracy and ITR in the online BCI experiments.

Subject	Accuracy (%)	ITR (bits/min)
S1	99.50	175.00
S2	95.50	160.64
S3	95.50	160.64
S4	90.00	144.14
S5	80.00	118.09
S6	95.00	159.04
S7	91.50	148.43
S8	97.00	165.63
S9	97.00	165.63
S10	78.50	114.48
Mean ±Std	91.95 ±7.22	151.18 ±20.34

4. Discussion

4.1 BCI performance

In this study, the EEG spectral analysis on amplitude and SNR showed rich and robust information of SSVEP harmonics (see figure 5). The frequency band of harmonics ranged from the fundamental frequency to an upper-bound frequency around 90Hz. To be noticed, although the amplitude of harmonics decreased sharply as the frequency increased, the SNR of harmonics remained at a relatively high level. This finding ensures that the harmonics can provide useful information for target identification. In addition, the SSVEP harmonics can largely reduce the detection errors caused by spontaneous EEG activities, which typically don't show any harmonic components (Birca et al., 2006). In offline data analysis using the standard CCA method, there was significant difference of classification accuracy between the numbers of harmonics for the reference signals (see figure 6). This finding differed from Bin et al. (2009)'s report. The difference could be due to different stimulus presentation methods and stimulus frequencies used in the two studies. In offline data analysis on estimating BCI performance, the FBCCA methods significantly outperformed the standard CCA method (see figure 8). Among the three FBCCA methods, M_3 showed the best performance. These findings suggest that, by decomposing SSVEPs into multiple sub-band components, the FBCCA method can efficiently extract the stimulus-driven information from the harmonics and thereby facilitate the frequency detection of SSVEPs.

The online BCI experiments with 10 subjects obtained an averaged ITR of 151 bits/min, to our knowledge, one of the highest ITRs reported in EEG-based BCIs. The present ITR is much higher than that of the 45-target speller obtained in Chen et al. (2014)'s study (105 bits/min). It is very close to the simulated ITR of the 32-target speller in Nakanishi et al. (2014b)'s study (167 bits/min), which used a mixed frequency and phase coding method. The ITR is also comparable to the BCIs based on code modulated VEPs (cVEP) (Bin et al., 2011; Spüller et al., 2012). Bin et al. (2011) reported an ITR of 108 bits/min in a 32-target BCI. Spüller et al. (2012) further improved the ITR to 144 bits/min by adopting an adaptive learning method. Due to non-stationarity and high individual variability, the cVEP and the SSVEP BCIs based on the mixed frequency and phase coding method always require system calibration before real system use. In contrast, the present BCI system uses sinusoidal

reference signals in the CCA process and thereby does not require any training data for individualized calibration. The nature of an unsupervised classification makes the proposed BCI system more practical for daily-life applications.

The BCI speller developed in this study achieved high performance at a spelling rate of 33.3 characters per minute. This spelling rate is comparable to the eye tracking-based spelling system, which typically has a spelling rate around 5-10 words per minute (Majaranta and Räihä 2007). Compared with the eye tacking system, a big advantage of the proposed system is that it does not require any calibration. In addition, the SSVEP BCI is more flexible regarding head movements, viewing distance, and gazing angle. However, towards practical applications, system performance, mobility, and user comfortableness of the proposed system require further improvements.

4.2 Design of a filter bank

To design a filter bank, the first step is to select the frequency range for SSVEP responses. In this study, the stimulation frequencies ranged from 8 Hz to 15.8 Hz. According to the SNR analysis (see figure 5), for each frequency, the harmonics exhibited clear peak frequencies of SNR within a wide range up to 90Hz. This study therefore selected a frequency range of 8-88Hz for filter bank design. To optimize the design of filter bank, this study proposed and compared three methods (M_1: sub-bands with equally spaced bandwidths; M_2: sub-bands corresponding to individual harmonic frequency bands; M_3: sub-bands covering multiple harmonic frequency bands). The bandwidth of 80Hz resulted in 10 sub-bands for these methods. Although all of the three methods covered the whole frequency band of 8-88Hz, the results suggested that M_3 can obtain the highest classification performance. The overlap of frequency range in the sub-bands might be more efficient to extract information in the harmonic components. Since the results for M_1 indicated the highest performance was obtained with eight sub-band components (i.e., 8-72Hz, see figure 8), this study further compared three different upper-bound frequencies (i.e., 72Hz, 80Hz, and 88Hz) for estimating BCI performance using M_3. The results showed comparable classification accuracy (72Hz: 88.22%; 80Hz: 88.95%; 88Hz: 89.47%). The accuracy of 88Hz was significantly higher than that of 72Hz and 80Hz (paired t-tests, $p<0.05$). However, the difference between 72Hz and 80Hz was not significant (paired t-test, $p>0.05$). This finding suggests an upper-bound frequency at 88Hz is suitable for the filter bank design in the proposed system that has stimulation frequencies within 8-15.8Hz. The second step in the filter bank design is to select the frequency band for each sub-band. In this study, the bandwidths for sub-band components in all three methods were determined according to the stimulation frequencies (i.e., 8-15.8Hz) and the proposed design strategies. For example, the frequency interval in M_1 was equal to the bandwidth of the stimulation frequencies (i.e., 8Hz). However, in practice, the design of filter bank is not limited by the stimulation frequencies. For example, different combinations of frequency ranges and frequency intervals can be used to further optimize the design of the filter bank.

4.3 Extended CCA methods using SSVEP training data

In several recent studies, extended CCA methods have been proposed to improve the standard CCA method for SSVEP detection (Pan et al., 2011, Zhang et al., 2014; Nakanishi et al., 2014b). These methods employed individual SSVEP training data to refine the reference signals in the CCA process. Pan et al. (2011) added a phase constraint to the reference signal by estimating the latency of SSVEP in the visual system with SSVEP training data. In Zhang et al. (2014)'s study, the multi-set CCA approach has been implemented with multiple trials from SSVEP training data. Nakanishi et al. (2014b) employed both sinusoidal reference signals and averaged SSVEPs as reference signals in CCA and then combined the features derived from multiple CCA processes. These methods all reported significantly improved BCI performance compared with the standard CCA method. However, compared with the standard method, the additional effort in collecting SSVEP training data increases the difficulty of system use. In general, a calibration session, which lasts at least several minutes, is required to collect training data for the extended CCA methods.

In contrast, the proposed FBCCA method does not require any training data. It simply uses a filter bank to decompose the SSVEP signals into sub-band components and then implement the standard CCA process for each sub-band component. As described above, the FBCCA method significantly outperformed the standard CCA method. The proposed method achieved very high accuracy (92%) and ITR (151 bits/min) in the online BCI experiments, which was very close to the BCI performance reported in Nakanishi et al. (2014b)'s study (accuracy: 91%; ITR: 167 bits/min). However, when sufficient training data are available, the BCI performance can be improved by adopting the extended CCA methods. For example, in a leave-one-out cross-validation, the method from Nakanishi et al. (2014b)'s study can obtain significantly improved classification accuracy (97% vs. 92%, $p<0.05$) and ITR (165 bits/min vs. 151 bits/min, $p<0.01$) using the same dataset from the present online experiments.

4.4 Computational cost

The standard CCA method has low computational complexity. However, compared with the standard CCA method, the proposed FBCCA method significantly increases the computational cost due to the inclusion of multiple standard CCA processes for the sub-band components (e.g., seven sub-band components used in the online experiment in this study). Since the feasibility of the FBCCA method in an online BCI highly depends on the computational cost, it is important to estimate the computational time for the FBCCA process. In this study, for a single-trial detection of SSVEPs, the computation time in the FBCCA process was around 40 milliseconds using MATLAB R2012b on Microsoft Windows 7 (with an Intel Cor2 Duo 2.4G processor). Note that, in CCA, the temporary variables related to the reference signals were calculated and saved before the online process. Besides, the temporary variables related to the testing trial were only calculated once before the following multiple CCA processes. Target identification in such a short time ensures the FBCCA method can satisfy the requirement of real-time execution in a high-speed BCI speller. The FBCCA method is also feasible for a mobile BCI system based on a portable data processing platform such as a smartphone (Wang et al., 2011).

4.5 Future work

This study developed a high-speed BCI speller based on the proposed FBCCA method and obtained an average ITR of 151 bits/min at a spelling rate of 1.8 seconds per character. Towards a practical BCI speller for real-life applications, the system needs to be further improved in the following directions. First, this study evaluated the system performance using a cue-guided spelling task, which allowed an interval of 0.55 seconds for gaze shifting. The copy spelling and free spelling paradigms (Spüller et al., 2012) should be used to evaluate the BCI performance in real practice. Besides, the gaze shifting time could be increased to make the system easy to use. Second, previous studies reported "BCI illiteracy" with the SSVEP-based BCI (Allison et al., 2010). Further investigations with a large number of subjects, especially patient subjects, are required to evaluate and improve the proposed method. Due to individual variability, system parameters such as electrode locations, stimulation frequencies, and frequency ranges for SSVEPs can be optimized for each individual to achieve the best system performance. Third, the low-frequency stimuli (8-15.8Hz) used in this study could lead to visual fatigue for some subjects. To reduce visual fatigue, the stimulation frequencies in the higher frequency band (e.g., >30Hz) can be applied (Chen et al., 2014). However, for high-frequency SSVEPs elicited by stimuli under a high refresh rate (e.g., 120Hz), the optimal frequency range for SSVEP harmonics still remains unknown. In addition to harmonics, the sub-harmonics might also be useful for target identification. Fourth, in addition to the signal-processing methods, performance of the SSVEP BCI could also be improved by advanced stimulus coding methods (Hwang et al., 2013; Gao et al., 2014) and system paradigms such as hybrid BCIs (Wang et al., 2014; Allison et al., 2014; Pan et al., 2014). Last, the proposed FBCCA method can also benefit target identification in the gaze-independent SSVEP BCIs, which are operated by visual selective attention (Kelly et al., 2005; Allison et al., 2008; Zhang et al., 2010).

Acknowledgments

References

Allison B Z, McFarland D J, Schalk G, Zheng S D, Jackson M M and Wolpaw J R 2008 Towards an independent brain–computer interface using steady state visual evoked potentials *Clin. Neurophysiol.* 119 399–408

Allison B Z, Luth T, Valbuena D, Teymourian A, Volosyak I and Graser A 2010 BCI Demographics: How Many (and What Kinds of) People Can Use an SSVEP BCI? *IEEE Trans. Neural Syst. Rehabili. Eng.* 18 107–116

Allison B Z, Jin J, Zhang Y and Wang X 2014 A four-choice hybrid P300/SSVEP BCI for improved accuracy *Brain-Comp. Interfaces* 1 17–26.

Ang K K, Chin Z Y, Wang C, Guan C and Zhang H 2012 Filter Bank Common Spatial Pattern Algorithm on BCI Competition IV Datasets 2a and 2b *Front Neurosci.* 6 39

Bin G, Gao X, Yan Z, Hong B and Gao S 2009 An online multi-channel ssvep-based brain-computer interface using a canonical correlation analysis method *J. Nueral Eng.* 6 046002

Bin G, Gao X, Wang Y, Li Y, Hong B and Gao S 2011 A high-speed BCI based on code modulation VEP *J. Neural Eng.* 8 025015

Birca A, Carmant L, Lortie A and Lassonde M 2006 Interaction between the flash evoked SSVEPs and the spontaneous EEG activity in children and adults *Clin. Neurophysiol.* 117 279–288

Boashash B 2003 *Time-Frequency Signal Analysis and Processing – A Comprehensive Reference*. Elsevier.

Brainard DH 1997 The psychophysics toolbox *Spat. Vis.* 10 433–436

Chen X, Chen Z, Gao S and Gao X 2014 A high-ITR SSVEP based BCI speller *Brain-Comp. Interfaces* 1 181–191

Cheng M, Gao X, Gao S and Xu D 2002 Design and implementation of a brain-computer interface with high transfer rates *IEEE Trans. Biomed. Eng.* 49 1181–1186

Friman O, Volosyak I, and Gräser A 2007 Multiple channel detection of steady-state visual evoked potentials for brain-computer interfaces *IEEE Trans Biomed. Eng.* 54 742-750

Gao S, Wang Y, Gao X and Hong B 2014 Visual and auditory brain-computer interfaces *IEEE Trans. Biomed. Eng.* 61 1435–1447

Herrmann C S 2001 Human EEG responses to 1–100 Hz flicker: Resonance phenomena in visual cortex and their potential correlation to cognitive phenomena *Exp. Brain Res.* 137 346–353

Hwang H J, Hwan K D, Han C H and Im C H 2013 A new dual-frequency stimulation method to increase the number of visual stimuli for multi-class SSVEP-based brain-computer interface (BCI) *Brain Res.* 1515 66–77

Kelly S P, Lalor E C, Finucane C, McDarby G and Reilly R B 2005 Visual spatial attention control in an independent brain-computer interface *IEEE Trans. Biomed. Eng.* 52 1588–1596

Lin Z, Zhang C, Wu W and Gao X 2007 Frequency recognition based on canonical correlation analysis for SSVEP-based BCIs *IEEE Trans. Biomed. Eng.* 54 1172–1176

Majaranta P and Räihä K J 2007 Text Entry by Gaze: Utilizing Eye-Tracking, In *Text entry systems: Mobility, accessibility, universality*, I. S. MacKenzie and K. Tanaka-Ishii, Eds., San Francisco: Morgan Kaufmann, 175–187.

Manyakov N V, Chumerin N, Robben A, Combaz A, van Vliet M and Van Hulle M M 2013 Sampled sinusoidal stimulation profile and multichannel fuzzy logic classification for monitor-based phase-coded SSVEP brain-computer interfacing *J Neural Eng.* 10 036011

Middendorf M, McMillan G, Calhoun G and Jones K S 2000 Brain computer interfaces based on the steady-state visual-evoked response *IEEE Trans. Rehabili. Eng.* 8 211–214

Müller-Putz G R, Scherer R, Brauneis C and Pfurtscheller G 2005 Steady state visual evoked potential (SSVEP)-based communication: impact of harmonic frequency components *J. Neural Eng.* 2 123–130

Nakanishi M, Wang Y, Wang Y T, Mitsukura Y and Jung T P 2014a Generating visual flickers for eliciting robust steady-state visual evoked potentials at flexible frequencies using monitor refresh rate *PLoS One*, 9 e99235

Nakanishi M, Wang Y, Wang Y T, Mitsukura Y and Jung T P 2014b A high-speed brain speller using steady-state visual evoked potentials *Int. J. Neural. Syst.* 24 1-18

Pan J, Gao X, Duan F, Yan Z and Gao S 2011 Enhancing the classification accuracy of steady-state visual evoked potential-based brain-computer interfaces using phase constrained canonical correlation analysis *J. Neural Eng.* 8 036027

Pan J, Xie Q, He Y, Wang F, Di H, Laureys S, Yu R and Li Y 2014 Detecting awareness in patients with disorders of consciousness using a hybrid brain-computer interface *J Neural Eng.* 11 056007

Regan D 1989 *Human Brain electrophysiology: Evoked potentials and Evoked Magnetic Fields in Science and Medicine*. Elsevier.

Russo F D and Spinelli D 1999 Electrophysiological evidnece for an early attentional mechanism in visual processing in humans *Vision Res.* 39 2975–2985

Spüler M, Rosenstiel W and Bogdan M 2012 Online adaptation of a c-VEP brain-computer interface (BCI) based on error-related potentials and unsupervised learning *PLoS One* 7 e51077

Vetterli M 1992 Wavelets and filter banks: theory and design. *IEEE Trans. Signal Process.* 40 2207 – 2232

Vialatte F B, Maurice M, Dauwels J and Cichocki A 2010 Steady-state visually evoked potentials: Focus on essential paradigms and future perspectives *Prog. Neurobiol.* 90 418–438

Wang M, Daly I, Allison B Z, Jin J, Zhang Y, Chen L and Wang X A new hybrid BCI paradigm based on P300 and SSVEP *J Neurosci Methods.* in press

Wang Y, Wang R, Gao X, Hong B and Gao S 2006 A practical VEP-based brain-computer interface *IEEE Trans. Neural Syst. Rehabili. Eng.* 14 234–240

Wang Y, Gao X, Hong B, Jia C and Gao S 2008 Brain-computer interfaces based on visual evoked potentials: feasibility of practical system design *IEEE EMB Mag.* 27 64–71

Wang Y, Wang Y T and Jung T P 2010 Visual stimulus design for high-rate SSVEP *Electron. Lett.* 46 1057–1058

Wang Y T, Wang Y and Jung T P 2011 Acell-phone based brain-computer interface for communication in daily life *J. Neural Eng.* 8 025018

Wolpaw J R, Birbaumer N, McFarland D J, Pfurtscheller G and Vaughan T M 2002 Brain–computer interfaces for communication and control *Clin. Neurophysiol.* 113 767–91

Zhang D, Maye A, Gao X, Hong B, Engel A K and Gao S 2011 An independent brain–computer interface using covert non-spatial visual selective Attention *J. Neural Eng.* 7 016010

Zhang Y, Zhou G, Jin J, Wang X and Cichocki A 2014 Frequency recognition in SSVEP-based BCI using multiset canonical correlation analysis *Int. J. Neural Syst.* 24 1450013